The Generalised Oscillator-Strength Density of the Helium Atom, Calculated by a New Implementation of the Complex-Coordinate Method *

Alejandro Saenz and Wolf Weyrich
Fakultät für Chemie, Universität Konstanz, Konstanz, Germany

Z. Naturforsch. **48a**, 243–250 (1993); received April 25, 1992

We report a calculation of the generalised oscillator-strength density (GOSD) of the helium atom for low momentum transfer. The calculation was performed by extraction of the searched entity from the resolvent of the complex-rotated Hamiltonian. That Hamiltonian was found using a standard ab-initio program without any change in the program code. The shape of the Bethe surface is reproduced (including resonances and the absorption edge). However, with increasing momentum transfer the magnitude of the calculated values for the Bethe ridge becomes too small. This is clearly demonstrated by an evaluation of the Bethe sum as a function of the momentum transfer. A comparison with recent additional theoretical data shows that the deviations are due to the employed basis set.

Key words: Generalised oscillator-strength density; Complex scaling; Bethe surface; Ab-initio calculation; Inelastic scattering.

1. Introduction

The original motivation for this work originates from the fact that the measurement of Compton spectra has reached such an accuracy that deviations from the currently employed theoretical model describing the scattering process (the sudden-impulse approximation) become more and more evident. This can be seen, e.g., from the discussion concerning the "Compton defect" [1–13].

It has been shown by Flores-Riveros, Froelich and Weyrich [8, 9] that the generalised oscillator-strength density (GOSD) can be extracted from the resolvent of the complex-rotated Hamiltonian of the target system. The GOSD, defined within the Bethe theory, quantitatively describes photoionisation as well as photon and electron scattering by atomic (target) systems under validity of the first Born approximation. When the GOSD is known, the double-differential and the total cross-sections are directly accessible. The complex-rotation procedure avoids the singularities of the resolvent and therefore renders the correct description of the resonances possible. If the GOSD is calculated in this way, the projectile-target interaction is included in first order and the Coulombic influence of the target to all orders. Therefore, the result is equivalent to the distorted-wave Born approximation (DWBA). If the resolvent is expanded in CI eigenfunctions, electron–electron correlation is also included in the calculation.

Since this method approaches the problem from the side of bound states, it is natural to perform the first tests of the method at values of low momentum transfer K and energy transfer E, although this part of the Bethe surface is not the aim of a typical Compton experiment using photons as projectiles. As typical examples to be mentioned, the use of MoKα radiation under nearly backward-scattering conditions leads to a cut through the Bethe surface at $K \approx 9\,a_0^{-1}$ and the use of the γ-radiation of a ^{241}Am source to a cut at $K \approx 29\,a_0^{-1}$. Therefore, there are no experimental Compton-scattering data for low K and E available at present. However, radiation sources of lower energy and/or smaller scattering angles can probe the Bethe surface also at values of low momentum and energy transfer.

At the same time, there exists a number of data in the range of small momentum transfer ($K \approx 0.2$ to $4.0\,a_0^{-1}$) measured by inelastic electron scattering experiments, especially for the helium atom. The importance of helium is due to the fact that helium is the

* Presented at the Sagamore X Conference on Charge, Spin and Momentum Densities, Konstanz, Fed. Rep. of Germany, September 1–7, 1991.

Reprint requests to Prof. Dr. Dr. h.c. W. Weyrich, Lehrstuhl für Physikalische Chemie I, Fakultät für Chemie, Universität Konstanz, Postfach 55 60, D-W-7750 Konstanz, Fed. Rep. of Germany.

0932-0784 / 93 / 0100-0243 $ 01.30/0. – Please order a reprint rather than making your own copy.

simplest example for a scattering problem that cannot be solved analytically. It therefore serves as a standard for electron scattering experiments. Kim [14] has compiled a number of different data sets with the aim to obtain consistent reference data. In addition, he compared those data with the best theoretical data available at that time. The discrepancies that were still contained in that data set motivated two groups [15, 16] to measure new data in a systematic way with two different detector systems. More recently Rudd [17] combined all these data sets in order to extract a new reference data set.

A large amount of theoretical work in this area, especially during the last fifteen years [18], is motivated by the discrepancies between the measured data sets, the problem of measuring absolute values, the need for extrapolation to scattering angles that are not accessible experimentally, and the wish to understand the scattering process in more detail. Beside the calculations at the level of the impulse approximation there exists a number of calculations (mostly of the triple-differential cross-section of the (e, 2e) experiment) at the level of the distorted-wave Born approximation (e.g. [19–24]) and even at the level of the second Born approximation [25–27]. The exact range of the validity of the DWBA, however, is still unknown, mainly owing to the dependence of the results on the chosen ansatz for the continuum wave function. For that reason a calculation of the GOSD of the helium atom applying the method of Froelich et al. [8] is desirable, since no ansatz for the continuum wave function has to be made, correlation between all electrons is included at the CI level, the calculated GOSD values are absolute values, and the case of multiple excitation of the target electrons is automatically included.

We have developed an implementation of the method that allows to perform the complex-scaled CI calculation in the atomic case using standard ab-initio programs without any change in the program code. No new types of integrals need to be calculated, and all optimisations of the ab-initio program used here (GAMESS [28]) are automatically included.

In a previous paper [29] we have given a detailed description of the method and have reported the calculated GOSD values in the optical limit (momentum transfer $K \to 0$). In the case of a not specially optimised basis set we have obtained values that can be regarded as satisfactory, when compared with experimental and other theoretical data. In this paper we report the results obtained with the same basis set in the case of low-momentum scattering for the helium atom. In the following section we give a brief outline of the theory. In the third section we report the obtained results and discuss the influence of the basis-set. The paper is concluded with an outlook to future improvements.

2. Theory

The complex-scaled atomic or molecular Hamiltonian $\hat{H}(\eta)$ [30–33] is obtained by multiplying the space coordinates of $\hat{H}(\boldsymbol{r}, \boldsymbol{R})$ with the complex number $\eta = \varrho\, e^{i\theta}$. In the case of atoms this procedure is obviously reduced to a scaling of the electronic coordinates $\boldsymbol{r}$ only. Because of the analytical structure of the atomic Hamiltonian, this scaling procedure can be performed at the CI level by a scaling of the kinetic-energy part of each matrix element by η^{-2} and of the potential-energy part by η^{-1}. Therefore the matrix elements have to be calculated only once when η is to be varied. This essential simplification is the so-called *direct approach* and was introduced by Doolen [34]. Usually, however, the kinetic and potential parts of the CI matrix are not directly accessible by standard ab-initio programs. In a previous paper [29] we have described a method how to extract this information with the aid of only two real-valued standard CI calculations. Once this information is obtained, the continuation of the matrix elements into the complex plane can be done using the direct-approach method. The resulting complex-symmetric matrix has to be diagonalised to give the eigenvalues and eigenvectors of the complex-scaled Hamiltonian. With the solution of the eigenvalue problem the GOSD is then accessible [8, 9] via the equation

$$\frac{\mathrm{d}f(E,K)}{\mathrm{d}(E/E_\mathrm{h})} = 2\,\frac{E}{(K a_0)^2}\,\frac{1}{\pi}\,\mathrm{Im}\left[\sum_{n=2}^{N}\frac{[\mathbf{c}_1^\eta]^T\,\mathbf{Q}_\eta^-\,\mathbf{c}_n^\eta\,[\mathbf{c}_n^\eta]^T\,\mathbf{Q}_\eta^+\,\mathbf{c}_1^\eta}{E_n^\eta - E_1^\eta - E}\right] \tag{1}$$

with $\mathrm{d}f(E,K)/\mathrm{d}(E/E_\mathrm{h})$ = generalised oscillator-strength density, E = energy transfer projectile to target, K = momentum transfer projectile to target, N = number of calculated CI states, $\mathbf{c}_i^\eta$ = eigenvector i of the complex-scaled CI eigenvalue problem, E_i^η = eigenvalue i of the complex-scaled CI eigenvalue problem, $\mathbf{Q}_\eta^\pm$ = matrix of the $e^{\pm ikr\eta}$-operator developed in the CI basis (configurations), $E_\mathrm{h} = 27.21\ \mathrm{eV} = 2hcR_\infty$, $a_0 = \hbar^2/m_\mathrm{e}e^2$.

The double-differential cross-section of photon or electron Compton scattering within the non-relativistic distorted-wave Born approximation (DWBA) can be calculated by

$$\left(\frac{\mathrm{d}^2\sigma}{\mathrm{d}\Omega\,\mathrm{d}E}\right)_{\mathrm{DWBA}} = C\,\frac{(\hbar K)^2}{E}\,\frac{\mathrm{d}f(E,K)}{\mathrm{d}E} \tag{2}$$

with

$$C = \frac{\omega_2}{\omega_1}\cdot\left(\frac{\mathrm{d}\sigma}{\mathrm{d}\Omega}\right)_{\mathrm{Thomson}} \tag{3}$$

in the case of photons and

$$C = \frac{k_2}{k_1}\cdot\left(\frac{\mathrm{d}\sigma}{\mathrm{d}\Omega}\right)_{\mathrm{Rutherford\ or\ Mott}} \tag{4}$$

in the case of electrons, where ω_i is the angular frequency of the photon and $p=\hbar k_i$ is the momentum of the electron. The subscript i is equal to 1 before and equal to 2 after the scattering event. A relativistic extension of (2) in connection with (3) has been given by Bonham [35]. In the case of (4), the factorisation implies either complete neglect or only approximate inclusion of the exchange between projectile and target when employing the Rutherford or the Mott cross-section, respectively.

In the limit $K\to 0$ the GOSD is equal to the dipole oscillator-strength density [36, 37]. For photon scattering the energy and momentum conservation laws result in the equation

$$K(\omega,\omega_1,\varphi) = |\boldsymbol{k}_1-\boldsymbol{k}_2| = (k_1^2+k_2^2-2k_1k_2\cos\varphi)^{1/2} \tag{5}$$

$$= \frac{1}{c}\left[\omega^2-2\omega_1\omega(1-\cos\varphi)+2\omega_1^2(1-\cos\varphi)\right]^{1/2}, \tag{6}$$

where $E=\hbar\omega$ is the energy transfer and φ is the scattering angle. From (6) it is obvious that even in the case of $\varphi\to 0$ the range of the Bethe surface that is accessible by inelastic photon scattering is restricted by

$$\lim_{\varphi\to 0} K = K_{\min} = \omega/c\,. \tag{7}$$

The case of electron scattering deserves special interest. Although it has been analysed by Inokuti [37] to some extent, approximations in his treatment make it advisable to present more rigorous relations here.

Also for electrons the smallest possible momentum transfer $p_{\min}$ for a given energy transfer E occurs at zero scattering angle. Then, in addition to the general formula

$$E = E_1 - E_2 = \sqrt{m^2c^4+p_1^2c^2} - \sqrt{m^2c^4+p_2^2c^2} \tag{8}$$

for the energy transfer, there holds

$$p_{\min} = p_1 - p_2 \tag{9}$$

for the momentum transfer, provided the target mass M is much greater than the electron mass m. Expressed in terms of dimensionless energies $\tilde{E}\equiv E/mc^2$ and momenta $\tilde{p}\equiv p/mc$, that minimal momentum transfer is

$$\tilde{p}_{\min} = \tilde{p}_1 - \sqrt{\tilde{p}_1^2 - 2\tilde{E}_1\tilde{E}+\tilde{E}^2} \tag{10}$$

$$= \frac{\tilde{E}_1}{\tilde{p}_1}\tilde{E} + \frac{1}{2\tilde{p}_1^3}\tilde{E}^2 + \frac{\tilde{E}_1}{2\tilde{p}_1^5}\tilde{E}^3 + \left(\frac{5}{8\tilde{p}_1^7}+\frac{1}{2\tilde{p}_1^5}\right)\tilde{E}^4+\ldots, \tag{11}$$

which becomes

$$\tilde{p}_{\min,\,\mathrm{non\text{-}rel}} = \frac{1}{\tilde{p}_1}\tilde{E} + \frac{1}{2\tilde{p}_1^3}\tilde{E}^2 + \frac{1}{2\tilde{p}_1^5}\tilde{E}^3 + \frac{5}{8\tilde{p}_1^7}\tilde{E}^4+\ldots \tag{12}$$

in the non-relativistic limit. The last equation and Inokuti's results [37] suggest that the momentum transfer could be made arbitrarily small with high momentum p_1 of the incoming electron. That is, however, not true, as the correct limit of (11)

$$\lim_{\tilde{p}_1\to\infty} \tilde{p}_{\min} = \tilde{E}\,, \tag{13}$$

shows. Its equivalence to (7) is obvious, when written in terms of absolute energy and momentum:

$$\lim_{p_1\to\infty} p_{\min} = E/c\,, \tag{14}$$

i.e. photon and electron scattering possess the same lower limit for momentum transfer for a given energy transfer. It is, however, remarkable that $p_{\min}$ obtained in the electron scattering experiment approaches the value of $K_{\min}$ of the photon scattering experiment (for the same energy transfer) only in the limit $p_1\to\infty$ and is greater otherwise, which can be seen from (11) also written in terms of absolute energy and momentum:

$$p_{\min} = \frac{E_1}{p_1c^2}E + \frac{m^2}{2p_1^3}E^2+\ldots \tag{15}$$

$$= \left(1+\frac{m^2c^2}{p_1^2}\right)^{1/2}\cdot\frac{E}{c}+\frac{m^2}{2p_1^3}E^2+\ldots\,. \tag{16}$$

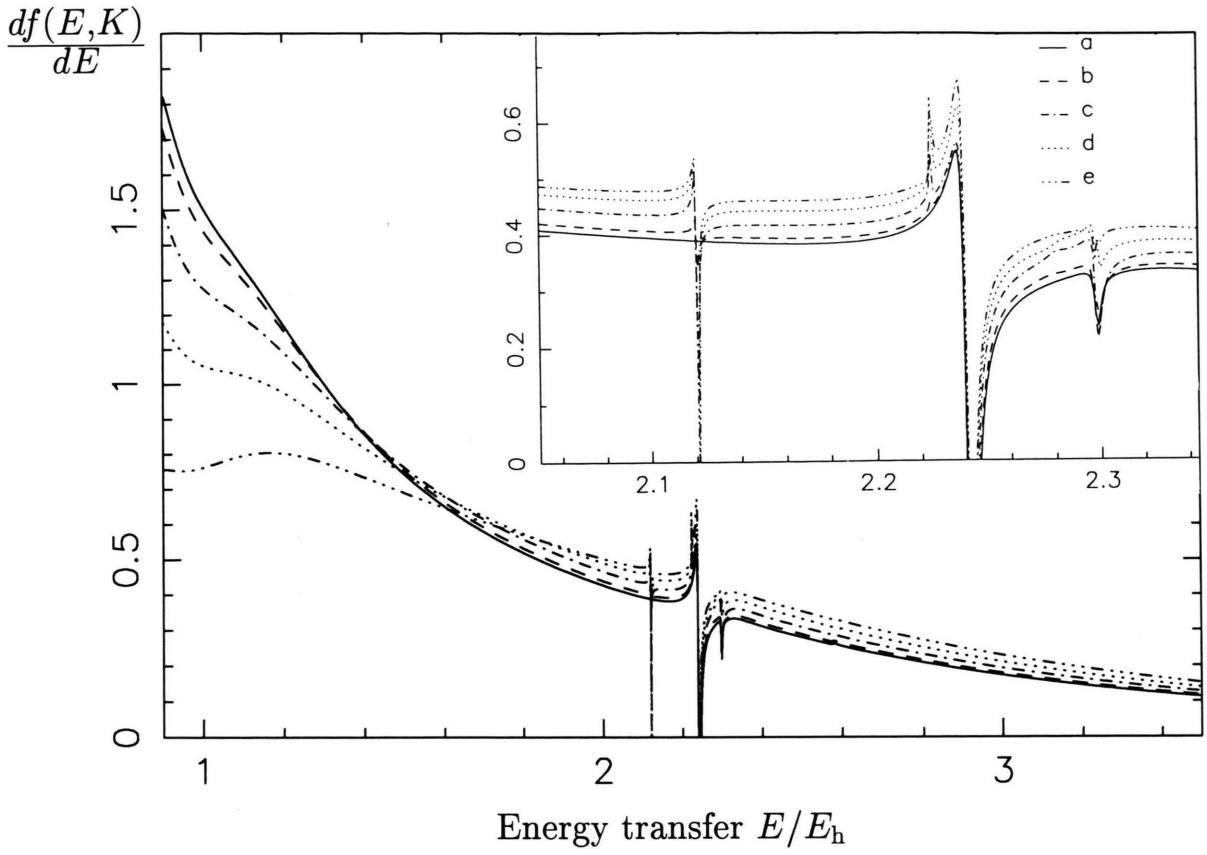

Fig. 1. Different cuts through the Bethe surface of helium at constant momentum transfer (K): a) $K \approx 0\ a_0^{-1}$, b) $K = 0.25\ a_0^{-1}$, c) $K = 0.5\ a_0^{-1}$, d) $K = 0.75\ a_0^{-1}$, e) $K = 1.0\ a_0^{-1}$. The resonant part of the spectrum is enlarged shown in the inlet. The complex-scaling parameter $\eta = \varrho\, e^{i\theta}$ is defined by $\varrho = 1.0$, $\theta = 24°$ in all five cases.

This means that the X-ray method can measure down to smaller values of K than the electron impact experiment does for any finite p_1.

Another interesting limit is the one for vanishing p_2,

$$\lim_{p_2 \to 0} \tilde{p}_{\min} = \sqrt{2\tilde{E} + \tilde{E}^2} \tag{17}$$

$$= \sqrt{2\tilde{E}}\left(1 + \frac{1}{4}\tilde{E} - \frac{1}{32}\tilde{E}^2 + \frac{1}{128}\tilde{E}^3 - \frac{5}{2048}\tilde{E}^4 + \ldots\right),$$

which lies above the limit given by (13) and approaches it for $\tilde{E} \gg 1$.

In our considerations here we have assumed inelastic scattering experiments on targets in the ground state, i.e. $E_1 > E_2$. Then, as we have shown, the dipole limit $K = 0$ is not directly accessible by any inelastic scattering experiment. Our finding, however, does not invalidate the analytical extrapolation also of experimental data over the forbidden gap to $K = 0$, just along the lines of Bethe theory [36, 37].

3. Results

We have calculated the GOSD for the helium atom in the case of low momentum transfer. The basis set used is the same as reported in [29]; it consists of 11 s- and 10 p-type even-tempered Cartesian Gaussians. 32 of the obtained 41 Hartree-Fock orbitals were chosen for a full CI calculation.

In Fig. 1 different cuts through the Bethe surface with constant momentum transfer are presented. The scaling angle θ was chosen to give the smallest θ-dependence of the spectra in this range of momentum transfer. In principle, the GOSD has to be stabilised for each value of E and K by varying the scaling

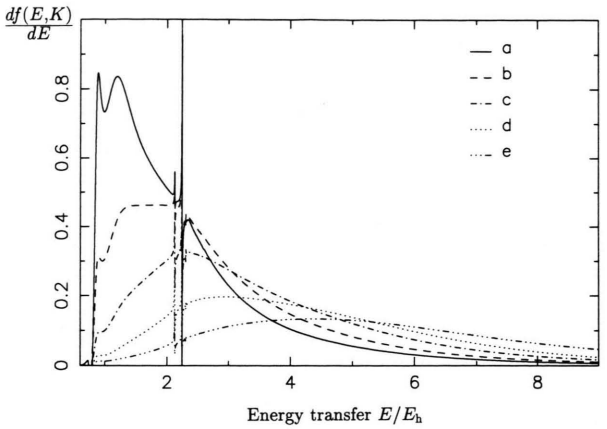

Fig. 2. Cuts through the Bethe surface of helium at constant – but in comparison to Fig. 1 higher – momentum transfer (K): a) $K=1.0\ a_0^{-1}$, b) $K=1.5\ a_0^{-1}$, c) $K=2.0\ a_0^{-1}$, d) $K=2.5\ a_0^{-1}$, e) $K=3.0\ a_0^{-1}$. The complex-scaling parameter $\eta = \varrho\, e^{i\theta}$ is defined by $\varrho = 1.0$, $\theta = 18°$ in all five cases.

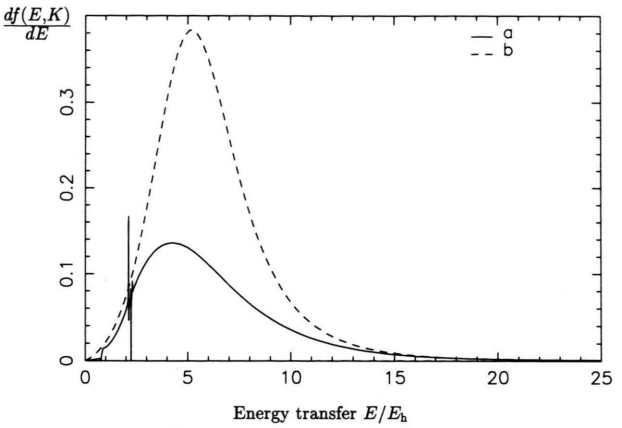

Fig. 3. Cut through the Bethe surface of helium at a momentum transfer $K = 3.0\ a_0^{-1}$; a) calculated in the distorted-wave Born approximation using the complex-scaling method ($\theta = 22°$), b) calculated in the plane-wave impulse approximation.

parameter η ($= \varrho\, e^{i\theta}$) separately. Since we were only interested in the general shape of the Bethe surface in this paper, we have not done such a detailed stabilisation procedure here and have rather restricted ourselves to a global stabilisation.

In Fig. 1 one can see the decrease of the maximum and its shift to higher energy transfer when the momentum transfer increases. The resonant part of the spectrum (which is shown enlarged in the inlet) demonstrates the automatic fulfilment of the dipole selection rules. S- and D-type resonances appear in the spectrum not before the momentum transfer becomes unequal to zero; in the dipole limit only P-type resonances are visible.

In Fig. 2 we present cuts through the Bethe surface at constant momentum transfer in the range from 1 up to $3\,a_0^{-1}$. The resonances and the absorption edge become less significant when the momentum transfer increases. At the same time the maximum shifts more and more to higher energy transfer, and its value decreases. These effects are in good agreement with the experimentally obtained Bethe surface [38].

In Figs. 3 and 4 we show spectra that were calculated by the method presented here for two values of momentum transfer in comparison to spectra that we have calculated in the sudden-impulse approximation. In the latter case the double-differential cross-section for the Compton process was calculated as a product of a theoretical Compton profile [39] and a function that is given by Opher et al. [40]. Then the GOSD was

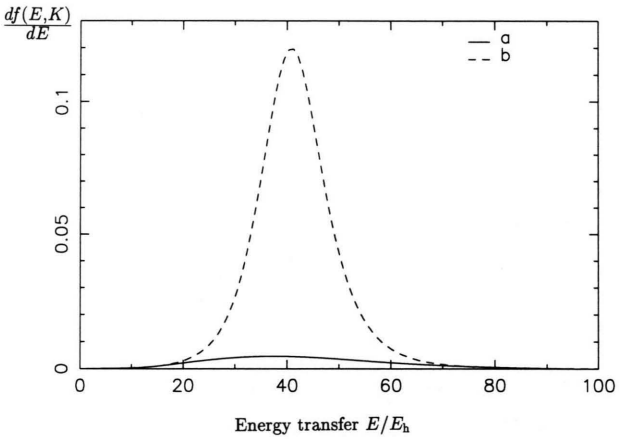

Fig. 4. Cut through the Bethe surface of helium at a momentum transfer $K = 8.98\ a_0^{-1}$; a) calculated in the distorted-wave Born approximation using the complex-scaling method ($\theta = 17°$), b) calculated in the plane-wave impulse approximation. In the maximum this is identical to the cut obtained in a Compton experiment using MoKα radiation.

obtained by an application of (2). The area under this curve is automatically normalised to the number of the electrons because of the use of a normalised theoretical Compton profile. Obviously the area under the respective curve calculated in the DWBA is smaller. On the other hand, the spectrum in the DWBA shows the absorption edge and the resonant features, which the impulse approximation cannot yield. In more de-

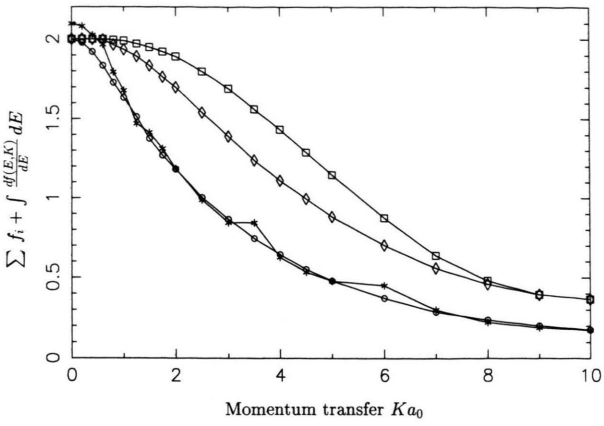

Fig. 5. Dependence of the values of the Bethe sum on the momentum transfer. ∗: Result obtained in this work with a basis set consisting of 11 s- and 10 p-type Cartesian Gaussians; ○, ◇, □: data calculated by a propagator method [41], ⊙: with a basis set consisting of 8 s- and 7 p-type Cartesian Gaussians, ◇: 8 s-, 7 p-, and 6 d-type Gaussians, □: 8 s-, 7 p-, 6 d-, 4 f-type Gaussians.

tail, the magnitude of the GOSD decreases too quickly with increasing momentum transfer.

A quantitative check of this observation is easily performed by a calculation of the so-called Bethe sum [36]

$$S(0, K) = \sum_{i=2}^{l} f_i + \int_{E_{\text{ion}}}^{\infty} \frac{\mathrm{d}f(E, K)}{\mathrm{d}E} \mathrm{d}E \,. \tag{18}$$

In this equation, l is the number of discrete states and f_i is the discrete generalised oscillator strength for the transition from the ground state into the discrete state i. E_{ion} is the first ionisation threshold of the system. The Bethe sum rule states that the Bethe sum is equal to the number of electrons of the system ($S(0, K) = Z$) for arbitrary momentum transfer K.

In Fig. 5 we display the obtained Bethe sums in dependence on the momentum transfer K. The discrete GOS values were obtained with the same program, modified in order to give the discrete GOS values as well as the continuous GOSD values. The discrete values were calculated with $\varrho = 1.0$ and $\theta = 0$. In the continuous case we have calculated the integral in (18) for different values of momentum transfer with ϱ varying in steps of 0.025 from 0.925 to 1.10 and θ varying in steps of 1° in the range of 6° to 28°. Then we have stabilised the Bethe sum numerically with respect to variation in η ($= \varrho\, e^{i\theta}$) for each momentum transfer. We have done this in order to be sure that the result is influenced by the scaling factor as little as possible. In fact, the result for a single fixed value of η shows a very similar behaviour – the curve contains only more oscillations with higher amplitude. From that result it can be seen that in our calculation the Bethe sum rule is approximately fulfilled only near the photoionisation threshold, independently from the scaling factor. With increasing momentum transfer the Bethe sum decreases very rapidly.

In a recent work by Mortensen et al. [41] the Bethe sum for the helium atom was calculated with a rather different approach using a basis-set-oriented propagator method. Also in these calculations Cartesian Gaussians were used. We have plotted the values (taken from Fig. 1 of the mentioned paper) for basis sets cointaining s- and p-, s-, p-, and d-type, and s-, p-, d-, and f-type Gaussians together with our result in Figure 5.

The comparison of the Bethe sum obtained with our calculation and the result of [41] obtained with a basis set with the same angular-momentum quantum numbers shows a remarkable agreement in spite of orbital exponents differing between the two basis sets. On the other hand, the results obtained within the propagator method with basis sets containing Gaussians of d- and f-type possess a larger range of momentum transfer in which the Bethe sum rule is fulfilled. These facts, in connection with the above-mentioned result of the approximate independence from the scaling factor η are, in our opinion, an obvious indication that the deviation from the Bethe sum rule with increasing momentum transfer originates only from the limited angular-momentum quantum numbers that were used in the basis set. The probable reason for this dependence is given by Mortensen et al. [41] by expanding the $e^{i\boldsymbol{K}\boldsymbol{r}}$-operator into a Taylor series. An equivalent explanation is given by Bonham [42] analysing the expansion of the GOSD into an even polynomial in K as it is used for the extrapolation of the measured data to $K = 0$,

$$\frac{\mathrm{d}f(E, K)}{\mathrm{d}(E/E_{\text{h}})} = A_0(E) + A_2(E)\, K^2 + \ldots + A_{2n}(E)\, K^{2n}. \tag{19}$$

Already the explicit form of $A_2(E)$ [42],

$$A_2(E) = \frac{|\langle 0|\, z_i^2\, |n\rangle|^2}{4} - \mathrm{Re}\left\{\frac{\langle 0|\, z_i\, |n\rangle\, \langle n|\, z_i^3\, |0\rangle}{3}\right\}, \tag{20}$$

demonstrates that higher angular momentum components must be involved because of the non-dipole selection rules in the quadrupole and octupole matrix elements.

4. Conclusions and Outlook

In this paper we have reported the results of a calculation of the GOSD of the helium atom in the low-momentum scattering regime. The calculation was performed using an implementation of the complex-scaling method, in which a standard ab-initio program is used without any change in the source code. No complex integrals were calculated to obtain the complex-scaled CI matrix.

The shape of the Bethe surface containing the absorption edge and the resonances is reproduced by the calculation, whereas the amplitude of the Bethe ridge decreases too rapidly with increasing momentum transfer. This was demonstrated by a calculation of the Bethe sum in dependence on the momentum transfer. The deviation is quite independent of the scaling factor used in the complex-scaling procedure. A comparison with Bethe sums calculated recently by a propagator method shows a very good mutual agreement when basis sets with the same angular-momentum quantum numbers are used in both procedures. It can therefore be concluded that the deviations depend solely on the angular-momentum quantum numbers of the basis set. The physical reason is that with increasing K the electron ejected in the inelastic scattering process is more and more directed parallel to the $\boldsymbol{K}$-vector; the contribution of that electron to the total wavefunction requires basis functions with high angular-momentum quantum numbers.

In further calculations, either much larger atomic basis sets will have to be employed (with the advantage of preserving the possibility to use a standard CI program) or new types of basis sets have to be introduced that take the preferred ejection direction of the outgoing electron into account. In the latter case, however, new computer codes will have to be developed.

Acknowledgements

We acknowledge the helpful discussion with J. R. Sabin about the basis-set dependence of the calculated GOSD and wish to thank E. H. Mortensen, J. Oddershede, and J. R. Sabin for making their data available to us prior to publication. We are grateful to R. A. Bonham for his advice concerning the equations (2)–(4) and the extrapolation of experimental GOSD data to zero momentum transfer, and for pointing out an error in (17). Further gratitude we owe to the Fonds der Chemischen Industrie for its continuous support.

[1] R. J. Weiss, Philos. Mag. **32,** 247 (1975).
[2] R. J. Weiss, M. J. Cooper, and R. S. Holt, Philos. Mag. **36,** 193 (1977).
[3] P. Pattison and S. Manninen, Philos. Mag. **36,** 1265 (1977).
[4] R. Hosemann, A. Müller, and D. Weick, Phys. Rev. Lett. **38,** 1211 (1977).
[5] A. D. Barlas, W. Rueckner, and H. F. Wellenstein, Philos. Mag. **36,** 201 (1977).
[6] W. Rueckner, A. D. Barlas, and H. F. Wellenstein, Phys. Rev. A **18,** 895 (1978).
[7] A. Lahmam-Bennani, A. Duguet, and H. F. Wellenstein, Chem. Phys. Lett. **60,** 411 (1979).
[8] P. Froelich and W. Weyrich, J. Chem. Phys. **80,** 5669 (1984).
[9] P. Froelich, A. Flores-Riveros, and W. Weyrich, J. Chem. Phys. **82,** 2305 (1985).
[10] F. Bell, J. Chem. Phys. **85,** 303 (1986), and further references therein.
[11] F. Bell, Z. Phys. D **3,** 97 (1986).
[12] A. Issolah, B. Levy, A. Beswick, and G. Loupias, Phys. Rev. A **38,** 4509 (1988).
[13] P. Holm and R. Ribberfors, Phys. Rev. A **40,** 6251 (1989).
[14] Y.-K. Kim, Phys. Rev. A **28,** 656 (1983).
[15] R. R. Goruganthu and R. A. Bonham, Phys. Rev. A **34,** 103 (1986).
[16] R. Müller-Fiedler, K. Jung, and H. Ehrhardt, J. Phys. B **19,** 1211 (1986).
[17] M. E. Rudd, Phys. Rev. A **44,** 1644 (1991).
[18] For a more detailed description of some of the different types of calculations see e.g. H. Ehrhardt, K. Jung, G. Knoth, and P. Schlemmer, Z. Phys. D **1,** 3 (1986).
[19] K. L. Bell and A. E. Kingston, J. Phys. B **8,** 2666 (1975).
[20] D. H. Madison, T. C. Calhoun, and W. N. Shelton, Phys. Rev. A **16,** 552 (1977).
[21] B. H. Bransden, J. J. Smith, and K. H. Winters, J. Phys. B **11,** 3095 (1978).
[22] R. J. Tweed, J. Phys. B **13,** 4467 (1980).
[23] A. Franz and H. Klar, Z. Phys. D **1,** 33 (1986).
[24] X. Zhang, C. T. Wheelan, and H. R. J. Walters, J. Phys. B **23,** L 509 (1990).
[25] A. Pochat, R. J. Tweed, J. Peresse, C. J. Joachain, B. Piraux, and F. W. Byron, J. Phys. B **16,** L 775 (1983).
[26] F. W. Byron, C. J. Joachain, and B. Piraux, J. Phys. B **19,** 1201 (1986).
[27] F. Mota Furtado and P. F. O'Mahony, J. Phys. B **22,** 3925 (1989).
[28] M. W. Schmidt, J. A. Boatz, K. K. Baldrigde, S. Kosecki, M. S. Gordon, S. T. Elbert, and B. Lam, QCPE Bulletin

7, 115 (1985). – M. Dupuis, D. Spangler, and J. J. Wendoloski, NRCC Software Catalog, University of California, Berkeley, CA 1980.
[29] A. Saenz, W. Weyrich, and P. Froelich, Int. J. Quantum Chem., in print.
[30] J. Aguilar and J. Combes, Commun. Math. Phys. **22,** 269 (1971).
[31] E. Balslev and J. Combes, Commun. Math. Phys. **22,** 280 (1971).
[32] B. Simon, Commun. Math. Phys. **27,** 1 (1972).
[33] B. Simon, Ann. Math. **97,** 247 (1973).
[34] G. D. Doolen, J. Nutall, and R. W. Stagat, Phys. Rev. A **10,** 1612 (1974).
[35] R. A. Bonham, Phys. Rev. A **23,** 2950 (1981).
[36] H. Bethe, Ann. Physik **5,** 325 (1930).
[37] M. Inokuti, Rev. Mod. Phys. **43,** 297 (1971).
[38] H. F. Wellenstein, R. A. Bonham, and R. C. Ulsh, Phys. Rev. A **8,** 304 (1973).
[39] P. E. Regier and A. J. Thakkar, J. Phys. B **18,** 3061 (1985).
[40] R. Opher, J. Felsteiner, and B. Lengeler, private communication (1976).
[41] E. H. Mortensen, J. Oddershede, and J. R. Sabin, Nucl. Instrum. Meth. B **69,** 24 (1992).
[42] R. A. Bonham, private communication (1992).